MARS VERTICAL AXIS WIND MACHINES

The Design of a Tornado Vortex Machine for Use on Mars

Work done under NASA Ames Grant No. NCC 2-710
Thomson Research Projects, Inc.
Lake Mills, Wisconsin
(A Non-Profit Organization)

Initial Design and Analysis done by Senior Engineering Mechanics and Astronautics Students at the University of Wisconsin-Madison, Wisconsin. May, 1991.

Davn Carlin
Amy Dyhr
Jon Kelly
J. Eric Schmirler
Mike Carlin
Won E. Hong
Kamin Mahoney

Analysis and Critique Completed June, 1994
by Mr. Owen Gwynne, Madison, Wisconsin.

ABSTRACT
MARTIAN TORNADO VORTEX WIND GENERATOR

Ever since Viking I and II landed on the surface of Mars in the summer of 1976, man has yearned to go back. But before man steps foot upon the surface of Mars, unmanned missions such as the Martian Soft Lander and Martian Sub-surface Penetrator will precede him. Alternative renewable power sources must be developed to supply the next generation of surface exploratory spacecraft, since RTG's, solar cells, and long-life batteries all have their significant drawbacks.

One such alternative is to take advantage of the unique Martian atmospheric conditions by designing a small scale, Martian Wind Power Generator, capable of surviving impact and fulfilling the long term (2-5 years), low-level power requirements (1-2 Watts) of an unmanned surface probe. After investigation of several wind machines, a tornado vortex generator was chosen based upon its capability of theoretically augmenting and increasing the available power that may be extracted from average Martian wind speeds of approximately 7.5 m/s.

The Martian Tornado Vortex Wind Generator stands 1 meter high and has a diameter of 0.5 m. Martian winds enter the base and shroud of the Tornado Vortex Generator at 7.5 m/s and are increased to an exit velocity of 13.657 m/s due to the vortex that is created. This results in a rapid pressure drop of 4.56 kg/s^2m across the vortex core which aids in producing a net power output of 1.1765 Watts.

The report of a Martian Tornado Vortex Wind Generator that follows, contains the necessary analysis and requirements needed to feasibly operate a low-level powered, unmanned, Martian surface probe.

EXECUTIVE SUMMARY

PROBLEM STATEMENT

Continued exploration of Mars is a NASA objective that will be met in the near future. Unmanned missions such as the Martian Soft Lander and Martian Sub-surface Penetrator will be used to gather information to aid in our understanding of the Martian environment, in hopes of one day establishing a manned outpost on Mars. Present day space-based energy sources (RTGs, solar cells, and long-life batteries) have significant drawbacks such as heat dissipation, limited hours of operation, and contamination effects, not to mention a major weight penalty for their long life. Thus an alternative renewable power source must be developed to supply the next generation of surface exploratory spacecraft. The Martian Tornado Vortex Wind Generator (MTVWG) is one such alternative energy source. The MTVWG derives its power from the Martian winds and is capable of feasibly operating a low-level powered, unmanned, Martian surface probe. This report summarizes a design proposal for a Martian Tornado Vortex Wind Generator.

BACKGROUND

Initially Mike Ralston proposed the idea of a Mars Wind Energy Conversion System to NASA-Ames last year. The objective of the proposal was to take advantage of the unique Martian atmospheric conditions by designing a small scale, Martian Wind Power Generator, capable of surviving impact and fulfilling the long term, low-level power requirements (1-2 Watts) of an unmanned surface probe.[27] His design was based upon the selection of a theoretical tornado vortex generator to augment and increase the available power that may be extracted from Martian wind speeds of approximately 7.5 m/s.

The proposal was subsequently accepted by NASA-Ames for a duration of two years and for an estimated 40,000 dollars in funding. The Martian Tornado Vortex Team is responsible for carrying out the first nine months of work. The objectives are as follows:

- Complete and document a literature search.
- Verify design requirements.
- Confirm the feasibility of power generation from Martian wind energy.
- Apply analytical and theoretical design methods to the development of a workable solution.
  - Detailed Mechanical Analysis
  - Design Optimization

Most of the work done on tornado-type wind energy systems was performed in the late 70s and early 80s during the energy crisis. A majority of the work was carried out by Dr. J. T. Yen of Grumman Aerospace and by Drs. Hsu and Ide of Iowa State. The advantage of their tornado-type wind energy systems over modern day windmills is that, "in addition to harnessing the wind's kinetic energy, it is also capable of deriving energy from the pressure field created by the vortex. Since the pressure energy is many times higher than the kinetic energy for a low speed wind, it follows that the amount of wind energy derivable would be many times higher than that for a conventional windmill."[28]

Substantial work has been done on devices that generate power from available wind sources here on Earth. However, there are few if any documented devices capable of extracting power from the Martian wind. The design of a Martian Tornado Vortex Wind Generator presented within this report attempts to rectify the preceding statement.

DESIGN PROCESS

In order to come up with a workable design for this project, it was first necessary to set a design schedule with milestones and objectives. An analysis of the project's needs and functions was done to more clearly define these objectives. The primary concern was with the harsh Martian environment, which is dislike that of the Earth's environment. Below, Table 1 summarizes a few of the major differences between Mars and Earth.

TABLE 1

PROPERTY	EARTH	MARS
Gravity	9.81 m/s^2	3.73 m/s^2
Pressure @ Surface	1013 mb	7.5 mb
Main Atmospheric Components	N_2, O_2	CO_2
Mean Temp. @ Surface	288 K	218 K
Solar Flux	1.37×10^6 erg/(cm^2 s)	0.59×10^6 erg/(cm^2 s)

The needs and functions were then used to create a FAST Diagram in order to highlight the critical needs of the project. Additional information was gathered and an extensive computerized literature search was conducted. With the gathered information, we proceeded to break down the MTVWG into its critical components. A preliminary design followed along with engineering analysis and design optimization. Finally conclusions were drawn upon and a final report written. Additional information can be found in Appendix A-1.

SUMMARY OF DESIGN

The Martian Tornado Vortex Wind Generator is constructed of four integral parts: the base, the shroud, the turbine blades, and the turbine shaft. A brief description of each part and its function is given below.

The base has the function of not only supporting the shroud and housing the turbine, but it also helps provide air feed into the turbine blades. While feeding the air into the turbine, the base increases the velocity of the air and thus increases the output potential of the generator. The base is constructed of an Aluminum-Boron Metal Matrix Composite and stands 0.3 m high. It is hollow and conical in shape with a minimum diameter of 0.224 m, a maximum diameter of 0.5 m, and a thickness of 0.01 m. The necking of the base increases the air inflow velocity from the average velocity of 7.5 m/s to 10.8 m/s. The overall mass of the base only was determined to be 9.706 kg.

The shroud is were the vortex is created and maintained. It is a circular tower consisting of a top and bottom plate holding 12

0.005 m thick fixed vanes in place and stands 0.7 m high. It accepts wind from all directions and its vanes are angled at 20° for maximum efficiency. The shroud has an outer diameter of 0.5 m and an inner diameter of 0.44 m at the top. The top plate and the vanes are made of Ti-5Al 2.5Sn and the bottom plate is made of Al/B Metal Matrix Composite. The total mass of the shroud was calculated to be 21.98 kg.

The shaft, or drive system, is the only moving component of the entire Martian Tornado Vortex Wind Generator. The drive system is a sort of floating shaft and turbine assembly which rises off of its base lip during operation. The shaft is composed of titanium with a maximum diameter of 0.0035 m and an over all length of 0.30 m. The ends of the shaft are conical to allow a single point of contact in the near frictionless jewel bearings. The turbine is fastened to the shaft through the use of splines and a reverse thread nut ensuring efficient torque transmittal and no possibility of failure. The total mass of the entire turbine-shaft assembly was calculated to be 0.0119 kg.

The rotor is the most critical component of the windmill. The rotor extracts energy from the wind and converts it into work energy. This work is used to turn the generator and produce power. The rotor is made of basically two components, the blades and the hub. The hub was addressed in the shaft analysis while the blades were addressed in the rotor analysis. The resulting airfoil has the following characteristics. The airfoil is NACA 23012. The span is 0.11 m. The chord length is 0.045 m. The airfoil has a built in twist represented by the equation $\theta = 82.567\text{-}1923.35+1.8949E4*r^2\text{-}6.8765E4*r^3$ with θ from the plane of rotation to the chord line. The blades are welded to the hub and the mass of the airfoils alone is $5.899x10^{-3}$ kg.

FINAL DATA

The final conclusions reached on the data required for further calculations are as follows:

Velocity of Martian Wind	7.50	m/s
Diameter of Shroud	0.50	m
Height of Shroud	0.70	m
Power Required with Efficiency	1.1765	kgm^2/s^3
Density of Martian Atmosphere	0.0156	kg/m^3

With the above values, the resulting data calculated for the general conditions of the Tornado Vortex Generator are shown below. The computations can be found in the Appendix B.

Circulation	$\Gamma = 11.781\ m^2/s$
Exit Velocity	$V_e = 13.657$ m/s
Turbine Radius	Rt = 0.112 m
Mass Flow	m = 0.0061 kg/s
Vortex Core Radius	a = 0.095 m
Tangential Velocity Component of the Vortex	$V_\theta = 19.737$ m/s
Pressure Drop Across the Vortex Core	$\Delta P_{ave} = 4.5577\ kg/s^2m$
Pressure Drop Across the Entire Turbine	$\Delta P_{turb} = 2.026\ kg/s^2m$
Total Mass	M = 31.70 kg

TABLE OF CONTENTS

ENTRY INTO THE MARS ATMOSPHERE 1
ACTUATOR DISC THEORY 2
PRELIMINARY CALCULATIONS 5
BASE 8
- INTRODUCTION 8
- FINAL DESIGN 8
- MATERIAL SELECTION 10
- FORCE ANALYSIS 12
- MASS ANALYSIS 15

SHROUD 16
- VANE SELECTION 16
- OVERALL ASSEMBLY OF THE SHROUD 17
- STRESS ANALYSIS 18

TURBINE SHAFT DESIGN 22
- INTRODUCTION 22
- MATERIAL SELECTION 22
- SHAFT OPERATION 22
- TURBINE ATTACHMENT 24
- TORQUE TRANSFER 25
- SHAFT ANALYSIS 26
- FINAL DESIGN OF SHAFT ASSEMBLY 28
- JEWEL BEARINGS 29
- MASS ANALYSIS 29

ROTOR DESIGN 30
- INTRODUCTION 30
- AIRFOIL THEORY 30
- AIRFOIL SELECTION 31
- TIP SPEED SELECTION 32
- AIRFOIL CHORD SELECTION 32
- AIRFOIL CHARACTERISTICS 33
- AIRFOIL ANALYSIS 34
- MASS ANALYSIS 35

AEOLIAN EFFECTS 36
EXPERIMENTAL & THEORETICAL RESULTS 38
- EXPERIMENTAL RESULTS 38
- THEORETICAL RESULTS 39
- COMPARISON WITH MOD-2 39

RECOMMENDATIONS & CONCLUSIONS 40
REFERENCES 41
APPENDICES TABLE OF CONTENTS 44

ENTRY INTO THE MARS ATMOSPHERE

Entry of the Martian Tornado Vortex Wind Generator through the Martian atmosphere is incomplete at this time, but it will be briefly highlighted below. The analysis will be modeled after the Martian Egg Probe Designs of 1989 &1990. (REF #8)

- The MTV will be protected by an ablative aeroshell which dissipates most of the heat generated by friction through the atmosphere during entry.
    - Aeroshell is made of nylon phenolic material.
    - Similar to the shielding used on the Galileo Probe.
- A ballute and parachute system is used as a first and second stage in slowing the MTV during its descent.
    - Aeroshell is discarded when parachute opens. The drag forces encountered are large enough to shear off the latches holding the aeroshell in place.
    - The ballute is a Kapton polymide balloon contained within a Kevlar 49 aramid fiber mesh.
    - The parachute is made of an uncoated Dacron 52 (polyester) material for the canopy and Kevlar 49 aramid fiber for the suspension lines
- The design terminal velocity of the entire entry system is less than 10 m/s at the surface of Mars.

ACTUATOR DISC THEORY

To better understand the unique advantages of the tornado vortex windmill we must first understand the basic principles behind rotor power absorption. The method used to do this is called Actuator Disc Theory and it was first used by Betz in windmill analysis.

The theory is based on the following assumptions:

- Steady homogeneous wind
- No obstruction of the wind either upstream or downstream
- Uniform flow velocity at the disk
- Incompressibility of the fluid
- No rotation of flow produced by the disk

The basic setup for analysis is shown below.

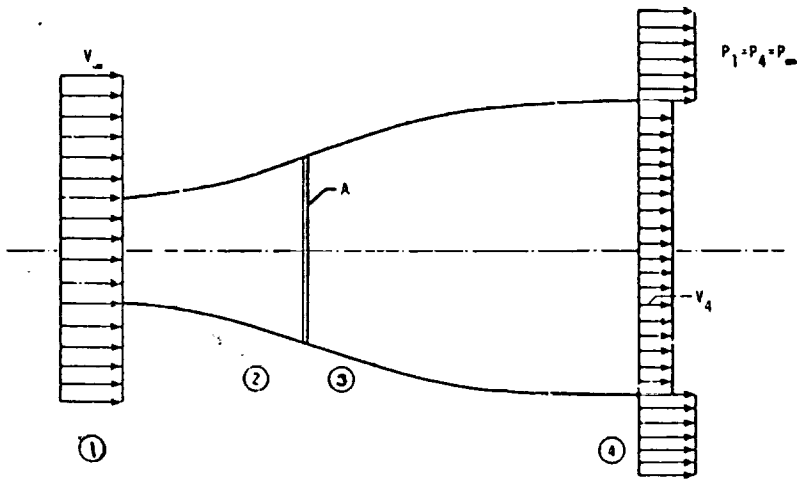

This theory uses an actuator disc to represent a turbine, across which characteristic pressure and velocity changes occur. The control volume in the figure above is cylindrical in shape with the assumption that air may only enter and exit on the left and right sides respectively. There are also four designated sections. Section one represents the free stream conditions with V_0 being the free stream velocity. Section two and three represent the conditions before and after the actuator disc with A designating the discs area. Finally section four represents the exhaust region of the flow.

In the analysis continuity gives us

$$V_2 = V_3$$

And the resultant thrust forces the disc 'sees' is

$$\text{(Thrust)} \quad T = \text{density} * A * V_4(V_1 - V_2)$$

Now applying Bernoulli's equations before and after the disc...

$$1/2*\text{density}*V_1^2 + P_o = 1/2*\text{density}*V_3^2 + P_3$$
$$1/2*\text{density}*V_2^2 + P_o = 1/2*\text{density}*V_4^2 + P_o$$

We solve for P_o and combine the result. Then solve for P_2 and P_3 to get:

$$P_3 - P_2 = \text{density}/2(V_4^2 - V_1^2)$$

This equation shows the pressure drop across the disc and its relation to the change in kinetic energy of the wind. The Power developed by this pressure drop is given by

$$\text{Power} = (P_2 - P_3)\, V_2 A$$

Combining these equations we get the power related to the kinetic energy.

$$\text{Power} = \text{density}*V_2 A/2(V_1^2 - V_4^2)$$

Note that (density*V2A) is equivalent to mass flow thru the disc area A. Through manipulation of these equations (see Appendix E "Actuator Disc Theory") we obtain the ratio of power extracted by the turbine to the kinetic energy of the free stream. This is called the coefficient of power. However, there is a limit to the amount of energy that can be extracted from the wind. This theoretical limit is known as the Betz limit.

$$\text{(Coefficient of Power)} \quad C_p = \text{Power}/(1/2*\text{density}*V_1^3*A)$$

Betz limit = C_p max = .59259

The Betz limit basically says that no more than 59% of the available kinetic energy in the wind may be extracted and converted

MARTIAN TORNADO VORTEX TEAM

into power. In addition this limit could only be reached if all elements of the wind turbine were at 100% efficiency. If we could somehow surpass this limit. The use of wind power as an energy resource would greatly increase.

Looking back we see C_p depends on Power, which depends on the change in pressure across the disc, which in turn is related to the change in kinetic energy. This pressure /kinetic energy relationship is shown below.

$$P_3 - P_2 = \text{density}/2(V_4^2 - V_1^2)$$

For us to surpass the Betz limit we must either increase the change in kinetic energy or increase the change in pressure. In the first case we are limited to changing the V_4 term because the V_1 term (free stream velocity) is not governed by our design. Yet by reducing this term we decrease the power available for extraction due to the decrease in mass flow. On the other hand there still exists the option to increase the pressure drop across the disc.

There are basically two ways which we could control the pressure drop across the disc. One way is to vary the aerodynamic parameters in our control. An example might be to vary the angle of attack of the turbine airfoil. A second method of varying the pressure drop is to place a low pressure region on the exhaust side of the disc. This is where the tornado vortex windmill comes in.

The tornado vortex windmill creates a vortex on the exhaust side of the disc or turbine. The vortex has a core that creates a low pressure exhaust region for the turbine. This in turn increases the pressure difference across the turbine. This pressure difference increases the amount of power that can be extracted which increases the coefficient of power. While this solution does not significantly reduce the mass flow. Some theoretical calculations have projected coefficients of power as high as 30 giving the tornado vortex windmill a very promising outlook.

PRELIMINARY CALCULATIONS

To begin our detailed design we first had to determine the governing parameters on which to base our optimizations. These parameters included tower height, tower width, design wind speed, turbine dimensions, vortex characteristics and so on.

Through research, it was discovered that the efficiency of the turbine and the vortex pressure difference advantage relied heavily on the vortex core size. Apparently the core radius could be no smaller than the turbine radius. If vortex core were to contract to a radius smaller than that of the turbine we would lose our advantageous low pressure region to disturbances from the exhausting turbine flow. Knowing this we proceeded with our design.

In the preliminary calculations we had to determine our environmental conditions of which wind speed was the first priority. We obtained a value of 7.5 m/s for the average wind speed from source [27] which we took to be our design speed. We then planned to use this value to find the resultant vortex core radius. Once the core radius was determined the turbine would be fitted to that radius. To start the number crunching we decided to limit the total height of the windmill structure to one meter so that we had a limiting factor. From this we could make relevant decisions regarding other dimensions. With the one meter parameter we chose some tower dimensions from which to begin. These values would later be optimized to fit our needs. The values chosen were a tower height of 0.7 meters and a diameter of 0.4 meters. The tower height dimension ended up being a permanent figure because of the lack of governing equations. The only relevant information on tower height was that the ratio of tower height to tower diameter be greater than one. On the other hand, tower diameter was intended to be optimized.

Once these values were set we began to calculate the relevant data with the following assumptions:

- The vortex is of an ideal configuration
- The velocity inside the tower walls is approximately the free stream velocity.

The basic vortex configuration is given below.

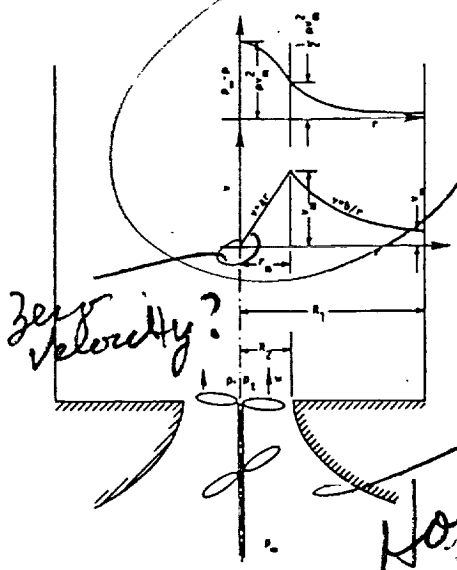

On the figure above are curves representing pressure drop across the radius and the velocity across the radius. Notice the large increase in the change in pressure near the center. This is the core region. It is in this core radius that we want to set our turbine radius.

In the Appendix E titled Initial Calculations the first part is devoted to deriving the coefficients of power and relating it to the diameter in an effort to later optimize the diameter. The second part entailed determining the resultant core size with respect to the given values for diameter and wind speed. It was here that we found two equations relating mass flow to our desired core radius.[20] The two equations were set equal to each other and solved for the core radius(R_1). see equation (1)

$$R_1 = (\sqrt{(2 \ln 2)}\ \Gamma_\infty / Ve\ 4\ \pi \qquad \text{equation (1)}$$

Where:

Ve = Exit velocity of the vortex from the top of the shroud

Γ = Circulation Strength

R_1 = Core radius

We also found that Power is related to the exiting vortex by equation (2)

$$P = \frac{\rho \Gamma Ve}{8\pi}$$ equation (2)

Where:

P = Power

ρ = Density

Solving this equation in terms of (Ve) we had all the required equations to find the core radius. We then tried a range of wind velocities from 5 m/s to 10 m/s to see what trends the core followed w.r.t. wind speed. As it turns out the core expands as the wind velocity increases. This is important because it allows the vortex to remain outside our turbine radius even if wind speeds increase. Wind speeds lower than the design speed tends to destabalize the core which results in a breakdown in the core pressure drop and an eventual collapse in power output. Plugging in our design wind speed of 7.5 m/s we calculated a vortex core radius at 0.04 m or 4 cm.

Next optimization of the diameter of the tower was carried out through manipulation of the previously found C_d equations and diameter of tower vs. diameter of the core ratios. It was found that the optimum diameter of the tower was approximately equal to the calculated diameter of the core. This result corresponded to sources which stated that the maximum power coefficient occurs at 2R1/D=1 (R1 equals core radius and D equal to tower diameter). One problem with having the core diameter equal to the tower diameter is that the windmill is limited to one wind speed. Any wind velocity greater than the design value would result in an unstable condition while any wind velocity less than the design value would also result in a unstable condition.

Therefore from these findings we decided to choose a tower diameter much larger than the core diameter of the design speed. This is so that with an increase in wind velocity the vortex core will be allowed to expand within the tower while still remaining stable.

BASE

INTRODUCTION

One of the most massive and most structurally demanding components of the Tornado Vortex Generator is the base. The base may seem very elementary, yet its functions are of great importance to the design and operation of the Tornado Vortex Generator. The function of the base is not only to support the shroud and house the turbine-shaft system, but it also provides the air feed into the turbine blades. While feeding the air into the turbine, the base increases the velocity of the air and thus increases the output potential of the generator. Other obvious functions of the base are to structurally withstand all adverse forces that the entire unit may encounter and protect all components from any environmental conditions that may be harmful. The following sections will discuss the overall design and its implications, material selection, force analysis, and the final mass analysis of the base design.

FINAL DESIGN

The final base design can be seen in Figure 1a and 1b. The first figure shows the outer view of a solid, smooth truncated cone like configuration with wind inlet ports at the bottom. The exact configuration is not a cone, but modeled by the following polynomial:

$$y = 19.968 - 2.5878x + 8.2927*10^{2}x^{2}$$

ok but why?

No relevant information was found as to what shape provides the optimum output, therefore the design was completed using an equation that provided a sufficient velocity increase to yield a satisfactory output. The inlet ports at the bottom are derived by the separation of the top from the bottom via solid cylindrical supports that measure 10 cm high with 2.5 mm radii. It was found that ten supports were sufficient to withstand all loadings. The overall outer dimensions of the base are shown on the figure.

what unit? what does this mean.

Figure 2 portrays the cross-sectional view of the base. This view reveals how the wind would flow through the base and into the

turbine blades. It can be seen that the wind enters through the ports and is directed upward into the turbine.

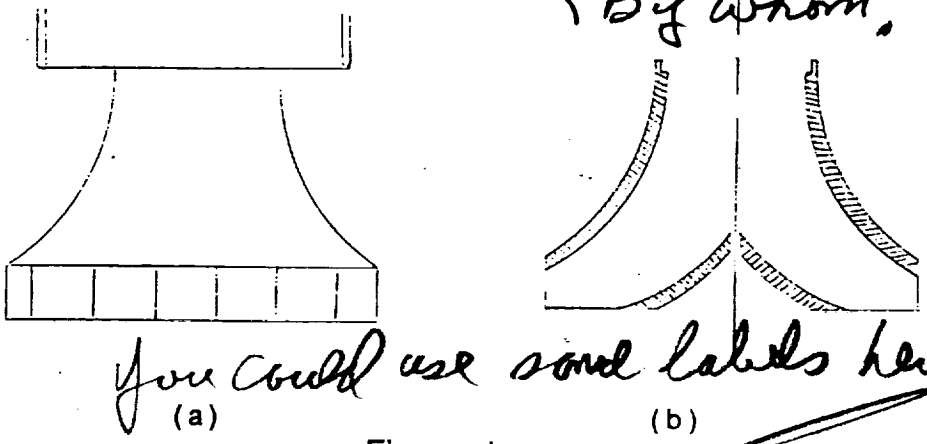

Figure 1

As the wind is tunneled upward, it is contracted due to the necking incorporated into the design. The necking was found to increase the inflow velocity from the average value of 7.5 m/s up to 13.44 m/s. This velocity increase is deceiving since no head loss was incorporated. As with any fluid flow, head losses originate as the wind is being tunneled upward. The conditions of head loss considered were those due to the overall fluid flow. entrance, contraction, bending, and exiting. The total head loss calculated was found to be 8.589 cm. Taking these losses into account, the final exit velocity was calculated to be 10.797 m/s. This final velocity was found to be sufficient in generating the one watt power requirement. The above values were computed utilizing the Bernoulli equation for fluid flow that is shown below:

$$\frac{P1}{\gamma} + \frac{V1^2}{2g} + z1 = \frac{P2}{\gamma} + \frac{V2^2}{2g} + z2 + \Sigma \text{head loss}$$

With this equation, the following assumptions were applied:

1. Constant density
2. Incompressible flow
3. One dimensional flow
4. Non-viscous flow
5. Steady flow
6. Irrotational flow

These assumptions were discussed thoroughly and found to be acceptable for our work. The complete calculations of the velocity increases, head losses and pressure differences can be found in Appendix B.

(a) (b)

Figure 2

Other features unique to the base design are the lip that is located on the inside of the top rim and the swirl molded into the bottom plate of the base. The lip, shown in Figure 2a, is cut into the upper rim and encompasses the entire circumference of the base. It measures 0.5 cm wide by 1.0 cm high. This lip serves the purpose of protecting the shaft system and its bearings from any crushing that may occur on impact with the planet. While the Tornado Vortex Generator is at rest, the turbine blades are actually resting on the lip. Thus when the unit is landing, the entire force of impact will be absorbed by the base rather than the bearings. When on the planet surface, the wind enters the unit and lifts the blades from their rest position and thus allows rotation. The swirl molded into the base bottom plate is shown in Figure 2b above. Experimental results show the optimum number of swirls to be one.[18] This swirl feature assists in directing the wind upward into the turbine blades and deters the tendency of merely exiting at the far side.

MATERIAL SELECTION

The material selection for the base is the most important step in the design process for this particular component. Two factors that needed to be considered throughout the selection process were one, the base will absorb all forces acting upon the Tornado Vortex Generator, and two, the base is the most voluminous component of the structure. Taking these two factors into consideration, along

with the obvious needs related to space travel and planet conditions the material selection was directed to the available composite materials. Considering the many composites on the market, the selection was narrowed to the Metal Matrix Composites (MMC) due to their following advantages over common metals and other composites:

1. Higher Strength /Density Ratio
2. Higher Stiffness/Density Ratio
3. Better High-Temperature Properties
4. Lower Coefficient of Thermal Expansion

The only disadvantages found regarding the MMCs were their higher cost, complex and expensive fabrication methods, immature technology and the fact that the only mature system on the market is the Al-B MMC.

The dominate matrix materials and system fibers used in MMCs are Aluminum-Boron, Aluminum-Graphite, Titanium-Boron, Magnesium-Graphite or any of the above using their alloys. The matrix-fiber system chosen was the Al-B configuration. Although each system has excellent qualities the choice to go with Al-B was made because of the fact that it is a better known system and thus more reliable than the other possibilities. Reliability is a major concern since no manpower will be available to provide maintenance while on Mars. It should also be noted that the Al-B MMC is in wide use within the space shuttle program. The trusses and other supporting members of the mid fuselage section and the cargo bay doors of the Space Shuttle Orbiter are comprised of a Al-B MMC.

The final choice was to implement the Al-B MMC with 50% Aluminum fiber content in a unidirectional configuration using only one ply. Some of the key properties of this Al-B MMC is shown below:

Longitudinal Tensile Ultimate	1490 MPa
Transverse Tensile Ultimate	138 Mpa
Longitudinal Compressive Ultimate	1725 Mpa
Transverse Compressive Ultimate	207 Mpa
Shear Ultimate	159 Mpa
Density	2710 Kg/m^3
Long. Coeff. of Thermal Expansion	6.1 $\mu m/m/^oC$
Trans. Coeff. of Thermal Expansion	21 $\mu m/m/^oC$

FORCE ANALYSIS

The base, being a major support, can be considered a pure compression member. The design was therefore based on preventing overall column buckling as well as local buckling. In optimizing the thickness of the member, the following buckling equations of a composite compression member were utilized:

$$\sigma \text{ opt} = \left[\frac{(\pi)(Exx)(\beta)(P)^2}{4L^2}\right]^{1/3}$$

$$r \text{ opt} = \frac{(P)(\beta)}{2(\pi)(\sigma \text{ opt})^2}$$

$$t \text{ opt} = \frac{(\sigma \text{opt})(r \text{ opt})}{(\beta)}$$

The values calculated with these equations yielded values so small that it was decided that any size larger would not increase buckling probability. The calculations for these decisions can be found in the Appendix B. The dimensions chosen were as stated previously and their performance will be discussed later when the force analysis is completed.

The driving forces acting on the base are the forces due to the weight of the entire system, the force at impact, the lift force caused by the tendency of the shroud to pull up due to the inner vortex action, and finally the continual drag force due to the wind on the outer surface of the component. A diagram showing how each force acts on the base is shown in Figure 3. The actual force calculations can be found in the Appendix B, a summary of the results are listed below:

Force of Impact	1005.55 N
Force of Weight	130.55 N
Force of Lift	0.0850 N/m
Moment due to Lift	0.0262 Nm
Force of Drag	0.1588 N/m

Analyzing the supports first, it is found that each support can be optimized down to a radius of 0.15 mm if ten supports were employed to carry the total reaction force of 1136.10 N. This is

obviously too small to work with, therefore a more practical and functional radius of 2.5 mm was chosen.

how about fewer supports?

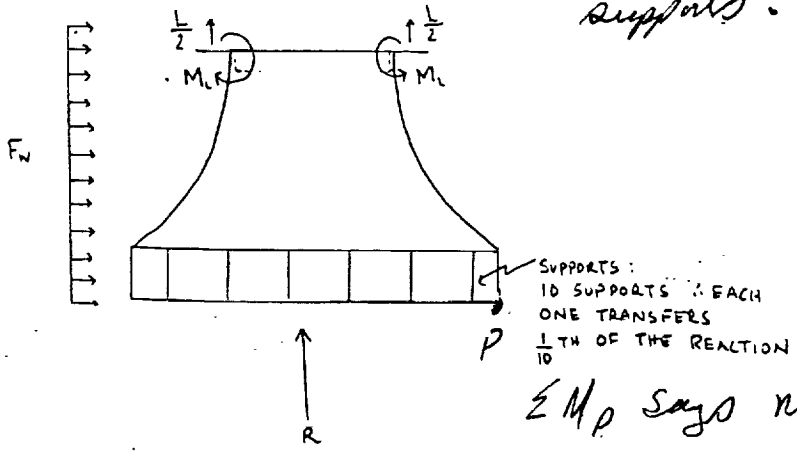

ΣM_P says not 1/10th each

Figure 3

Even with this value, and a factor of safety of 1.1 the overall stress placed on each support is found to be 5.7 MPa. This stress is not a concern to the design since the ultimate stress this material can withstand in compression is 1725 MPa. Buckling of the support members is analyzed with the use of the buckling equation noted earlier for composite materials. The overall buckling stress was calculated to be 0.705 MPa. This buckling stress is again no problem due to the robustness of the material used in manufacturing. With this analysis completed, the final dimensions of each support remains at 10 cm high with a radius of 2.5 mm since there is not any danger from the loads present. The complete calculations of these results can be found in the Appendix B.

what is a buckling stress?

seems like we can get rid of some weight here!

In analyzing the major portion of the base, two factors were closely evaluated. The first concern was the deflection or expansion of the top of the base due to the loading encountered. If the deflection or expansion was too high the base could interfere with the movement of the turbine blade. This concern is very important to the design because the tolerance between the blades and the inner base wall is on the order of millimeters. The second concern is buckling of the base walls under the forces it is confronted with. The following paragraphs with give the results of these concerns.

be more specific

The deflection of the top due to the edge loading caused by the lifting of the shroud is modeled by a distributed load encompassing the outer lip where the shroud is connected to the base. This distributed load is brought in to the base and thus modeled by a distributed moment acting on the upper edge of the base. This distributed bending moment acts to bend the base into the turbine blades. The theory used to deal with this phenomena utilized the long cylindrical shell theory.[9] The application of this theory is acceptable even though the base design is not "long", the base is viewed as mathematically long since $\lambda L > 2\Pi$. According to this theory, the largest meridional bending moment per unit length is 0.0262 Nm/m. With this loading the maximum radial deflection experienced by the base walls is found to act at the top and to be only 467.609×10^{-9} m. This radial deflection is accompanied by a maximum meridional rotation of -35.5×10^{-6} which also occurs at the top of the base. Together these produce a maximum circumferential membrane stress of 883.26 N. These results are not significant since they are so small. The deflection will not inhibit the turbine blades rotation and the circumferential membrane stress is not large enough to effect the component. A summary of the these results is shown below and the complete calculations can be found in the Appendix B.

Max. Meridional Moment	$M = 0.0262$ Nm/m
Max. Radial Deflection	$\omega = 467.609 \times 10^{-9}$ m
Max. Meridional Rotation	$\psi = -35.497 \times 10^{-6}$
Max. Circumferential Stress	$\sigma = 883.26$ N

The expansion of the base due to the drastic temperature changes on Mars also is analyzed to ensure that the base does not interfere with the turbine blades rotation. The most drastic temperature change was found to be 160 °C either way (hotter or colder). Using this, the following equations for thermal expansion of composites were utilized:

$$\alpha xx = Exx/\Delta T$$
$$\alpha yy = Eyy/\Delta T$$
$$\alpha xy = \gamma xy/\Delta T$$

Using these equations and the material properties of Al-B MMC, it is found that the midplane normal strains in the component were 3360, 976, and 0.0 µm/m respectively. These expansions are more of a

concern since they show that an expansion or contraction of 3.36 mm is possible. According to the turbine shaft system calculations this would not interfere with the operation of the turbine blades. The results of these calculations are shown below with the complete computation in the Appendix B.

Exx = 3360 μm/m
Eyy = 976 μm/m
γxy = 0.0 μm/m

The critical buckling stress of the base was found to be 20.63 MPa using the top (smallest) diameter and using the bottom diameter the buckling stress was calculated to be 20.56 MPa. Since both calculations came to be almost equal the assumption of modeling the base as a cylinder is verified. This critical buckling stress calculated is not a problem for the design since the material the base is manufactured from can easily accommodate these loads and the stress that it is feeling does not exceed 25.5 KPa. The local buckling critical stress was calculated to be about 4.46 MPa and no larger than 6.08 MPa. Again, this is not a problem since the stress felt by the base does not exceed 25.5 KPa. To view the computation of the buckling analysis see Appendix B

To complete the analysis on the base it should be noted that the drag force on the base structure due to the blowing wind yields a force of 0.0329 N. This force was considered negligible in the base analysis due to the small size.

MASS ANALYSIS

The mass analysis of the base was completed viewing each component separately and then summing results for the total mass of the base. The table below gives all pertinent data and actual calculations can be found the Appendix B.

PART	VOLUME	MASS
Lip	69.586×10^{-6} m^3	0.1886 Kg
Walls	0.001520 m^3	4.1192 Kg
Flat Bottom	0.001569 m^3	4.2519 Kg
Inner Swirl Cone	0.000423 m^3	1.1463 Kg
TOTAL	0.00358 m^3	9.706 Kg

SHROUD

VANE SELECTION

The shroud is one of the most important components of the tornado vortex windmill. It is where the vortex is created. There are two types of towers that we looked at.

1) Spiral Tower -stronger and more stable vortex
-only accepts wind from one direction

2) Circular tower -not as strong or as stable as spiral tower
-accepts wind from any direction

From these two types we chose the circular tower because it accepts wind from all directions and we will not have to direct it into the wind. On the circular tower there are two types of vanes.

1) Movable vanes - move and act similar to a spiral tower
   a) the vanes open in front to accept the wind
   b) and close on the back
   c) causing a spiral vortex type configuration

2) Fixed vanes
   a) fixed, always open
   b) they will accept wind from any direction
   c) they do not give us as intense or as strong vortex as the movable vanes.

From these two we chose the fixed vanes,.since it requires no maintenance and no moving parts which gives simplicity of the design.[31]

a very simplistic decision making process

Next, because we chose fixed vanes, we have to determine what angle to fix them at (angle tangent to the circumference of the shroud). From the theoretical study done by Miller it was found that a 45 degree angle gave the best vortex. However, later experimental data showed that 20 degree angle was the optimum angle for the vanes. Therefore, we will use a circular tower with fixed vanes at 20 degree angles.[15]

By whom. It is applicable

OVERALL ASSEMBLY OF THE SHROUD

The shroud structure consists of three major components: a top plate, vanes, and a bottom plate which is part of the base of the tower. The top and bottom plates hold 12 vanes in place at 20 degrees tangent to the circumference of the tower. The dimensions of these three parts are as follows:

	Outer Diameter	Inner Diameter
Top Plate	0.500 m	0.440 m
Bottom plate	0.500 m	0.214 m
Vanes (12)	0.005 m x 0.100 m x 0.700 m	

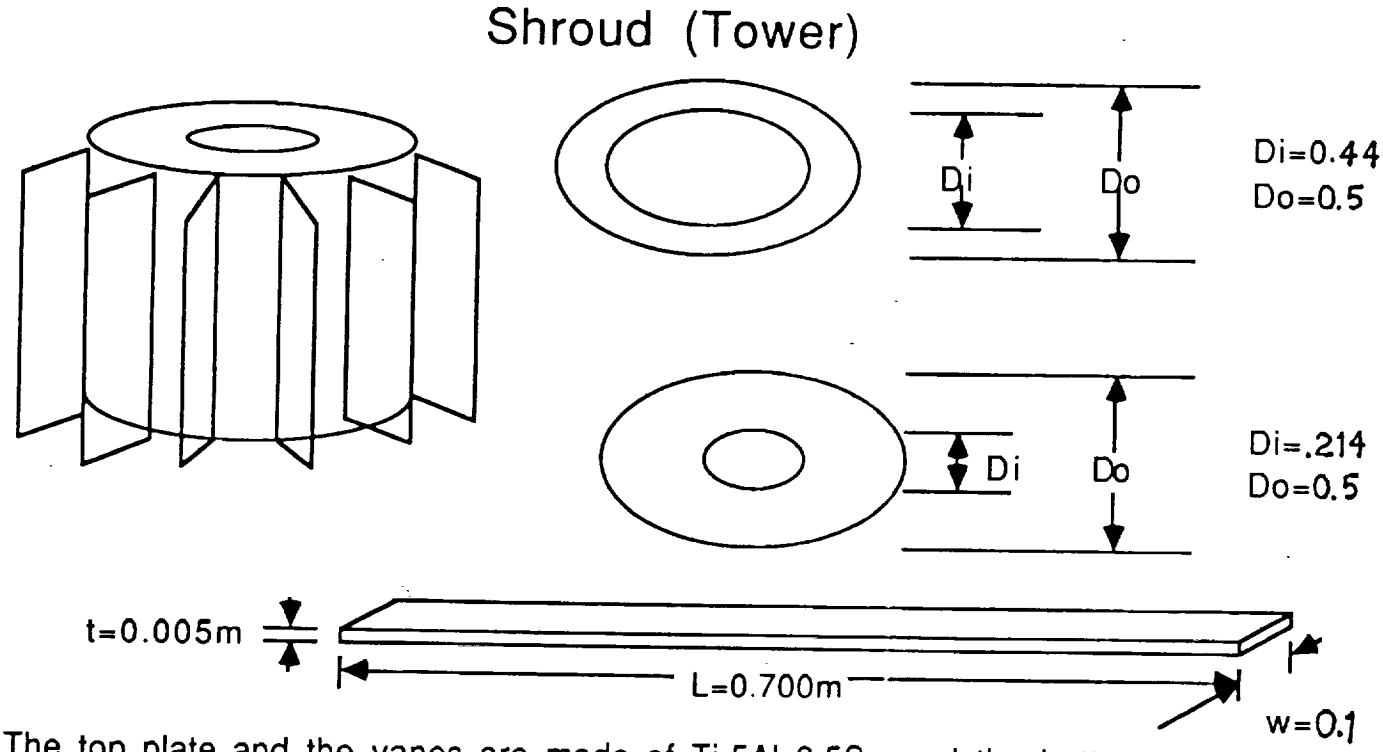

The top plate and the vanes are made of Ti-5Al 2.5Sn and the bottom plate is made of B/Al Metal Matrix Composite. The mass analysis of the structure is as follows:[33,6]

	Material	Mass(kg)	Earth wt.	Martian Wt.
Top Plate	Ti-5Al 2.5Sn	1.00	9.81	3.73
Vanes (12)	Ti-5Al 2.5Sn	18.81	184.5	70.16
Bottom Plate	B/Al MMC	2.17	21.29	8.09
Total		21.98	215.6	81.98

The bottom plate is formed in one piece with the base of the tower. The vanes and the top plate are welded together. The mass of the bottom plate does not include the base of the tower.

STRESS ANALYSIS

There are three major forces that are exerted on the shroud structure. There is a wind drag force, typically known as drag force, the weight of the structure, and the impact load. Among these three forces, the most significant force is the impact load. The following are the mechanical properties of Ti-5Al 2.5Sn.[33]

I would guess that last you should justify

Mechanical Properties of Ti-5Al 2.5Sn

	English Units	SI Units
Young's modulus	16 E6 psi	1.10 E11 Pa
Ult. Tensile Strength	120 E6 psi	8.27 E11 Pa
Comp. Yield Strength	110-120 E6 psi	7.58-8.27 E11 Pa
Shear Stress	100-110 E6 psi	6.89-7.58 E11 Pa
Density	0.162 lb/in^3	4480.66 kg/m^3

The impact load was calculated by using the impact force formula.[26] We found the typical impact velocity and impact time for landing the spacecraft.

What is this term?

$Ft=m(v+gt)$

define terms

$v = 10$ m/s
$t = 0.4$ s
$m = 35$ kg

who says?

From this, the impact load was calculated to be 1005.5 N (see Appendix C) with an assumption of total mass = 35 kg. With this impact load, two types of analysis were done to obtain a minimum thickness of the vane which will carry most of the compressive load. First, compressive yield stress was used to calculate the minimum thickness.[5] This calculation delivered a minimum thickness of t=1.105 E-9 m, which means any kind of reasonable thickness will withstand the compressive load. Secondly, a buckling test was done on the vanes; the total impact load of 1005.6 N was divided into 12 vanes which gave 83.8 N.[9] We used 100 N for a safety factor. This gave us the thickness of 0.0011 m.(See Appendix C) [5,9]

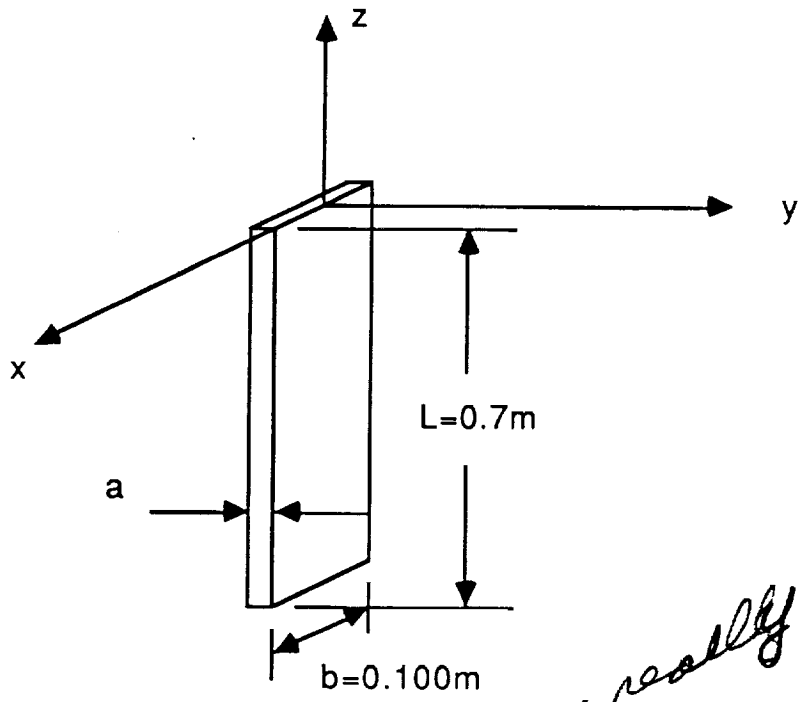

Critical Buckling Test (Both Ends Fixed) $\sigma cr=\pi 2*E/(Le/r_z)^2$ $Le=0.5L$ $r_z^2=a/12$

From these two results, it was clear that loads applied are not very significant. Therefore 0.005 m was chosen for the thickness of the vane. For safety reasons, a larger value for thickness was used even though the required thickness was only 0.0011m. The vanes now have a cross section of 0.100 m x 0.005 m. With this cross section, shear stresses on the vanes were calculated. The only force that contributes to the vanes' shear stress is the wind drag force. The drag force was calculated by treating the vanes as rectangular plates facing the wind. With an aspect ratio of 7, a C_D was determined to be 1.24. Thus the drag force applied to the vanes came out to be 0.124 N, and for each vane, the average drag force is 0.0103 N. However, each vane will experience different drag forces due to its orientation toward the wind. The middle vane has the most exposed area toward the wind and this maximum drag force is 0.0357 N which is more than three times the average drag force.[5,9,22]

Shear Stress due to Wind Drag

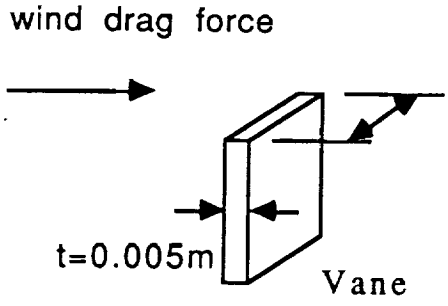

$\tau = P/A$

$A = w \times t$

$\delta = -q*L4/384*EI$

Ti-5Al 2.5Sn has a shear strength of 6.89-7.58 E11 Pa. Comparing a shear stress of 71.4 Pa with its ultimate shear stress, it was determined that wind drag force causes a negligible shear stress on the vane. Then deflection caused by the drag force was calculated, treating the wind as a uniformly distributed load. The maximum wind drag of 0.357 N caused 2.79 E-7 m deflection which is 0.28 μm. This was again accepted as a negligible deflection. Again, the calculations clearly proved that external loads does not cause any significant damage or deformation of the structure.(See Appendix C)[5,9]

Lastly, the stability of the structure was determined. One of the main concerns in this calculation was whether the structure will tip over or not. The two forces that were considered, were the weight of the structure and the wind drag on the whole structure. By assuming the projected area of the structure as a rectangular plate of 1.0 m x 0.5 m, the weight of the structure on Mars was calculated to be 114.25 N and the total wind drag was 0.263 N. Then a moment was taken about the right lower corner point A. As long as the moment about x-axis stays negative or 0, the structure will stay stable.

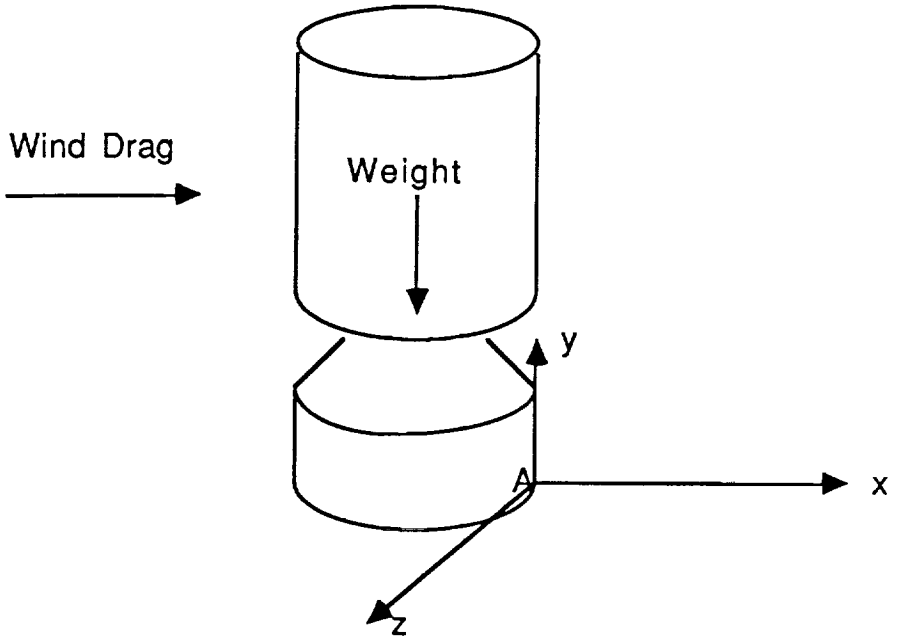

The calculated moment was -28.43 Nm, which means there are more forces keeping the structure on the ground than those opposing it. Therefore, the tornado vortex will withstand the landing impact, the weight of itself, and wind drag from any deformation or failure. Also, the structure will not tip over unless the wind speed increases up to 108.6 m/s.(See Appendix C)[5]

Yeah!

I seem to recall that this is a possibility; however, I suppose we could anchor it to the Lander.

TURBINE SHAFT DESIGN

INTRODUCTION

The shaft, or drive system, is the only moving component of the entire Tornado Vortex Generator. The design of the shaft was very extensive and all of the features have very important functions. The reasons for these features and their method of optimization will be discussed in the following pages.

MATERIAL SELECTION

A typical material selection for the shaft was done. First a list of all the important and required properties was noted. Using this list a couple of possible candidate materials were chosen because of their similar compatible characteristics. Each material's properties were listed and weighed for importance. After trade-offs were made the final selection of Titanium was made. The most important property in selection was the strength to weight ratio. Of the materials selected Titanium had the best and this was the major basis for its choice. This meant,of course, its density and strength were also very good. Another reason for its selection was because it had the best coefficient of thermal expansion which was also an important feature. This is because the temperature change on Mars is very great year round and our tolerances are very small. The procedure and data used in this process can be seen in Appendix D.

SHAFT OPERATION

The operating design of our drive system is a very unique one. We have designed a sort of floating shaft and turbine assembly. When the system is at rest the assembly rests on a lip built into the base.(see Fig. 4a) The end of the turbine blades rest on a 0.005 m lip leaving a 0.003 m gap between it and the wall. This was done to take away any compressive loading, and buckling, in the shaft. In doing this we could reduce the size of the shaft and avoid any load during impact being transmitted into the jewel bearings at the base which could possibly damage them. When in operation the entire

assembly is lifted off the edge due to a thrust load of 0.076 N on the turbine blades.(see Figure 4b) The lift of the assembly is controlled by three wires attached at the lip of the base to the top jewel bearing. These wires are initially relaxed and become taught when lifted and allow a 0.015 m gap between the turbine blades and the lip during operation.

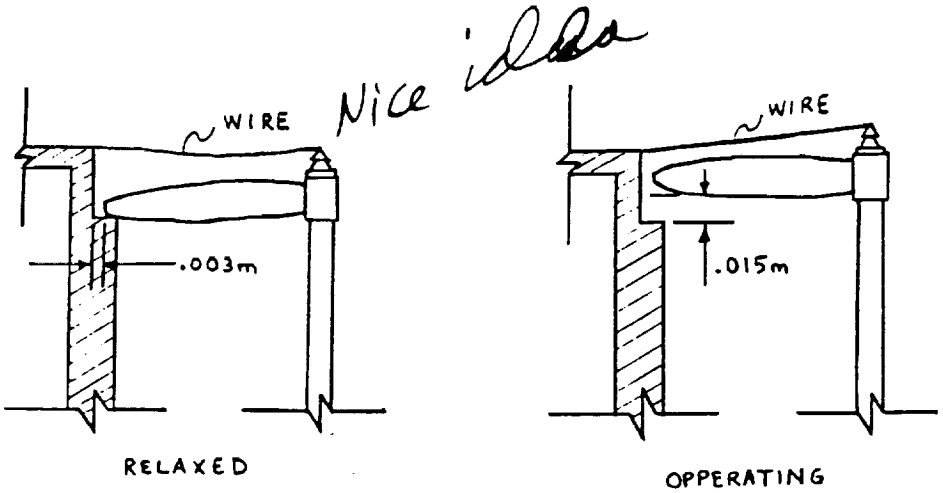

(a.) (b.)

Figure 4

The wires are made of solid titanium whose size was optimized using equation (1) and solving for the optimum diameter of the wires.

$$d_w^2 = \frac{4P}{\pi \sigma_y} \qquad \text{equation (1)}$$

Where:

d_w = Diameter of wire
P = 1/3*(Load due to thrust of turbine)
σ_y = Yield Strength (with F.S. = 1.1)
A = Cross-sectional area

The minimum wire diameter, using three wires, was found to be 1.38×10^{-5} m. Actual calculations can be found in Appendix D.

TURBINE ATTACHMENT

The turbine blades are welded to a hub and securely attached to the shaft through the use of a reverse treaded nut. Because of the specification of no maintenance reverse threaded nut was chosen to ensure tightening of the nut during operation. A normal threaded nut would possibly loosen causing the assembly to fail and extensive damage to occur. The stresses on the nut and the shaft due to the force of thrust of the turbine can be seen in Figure 5.

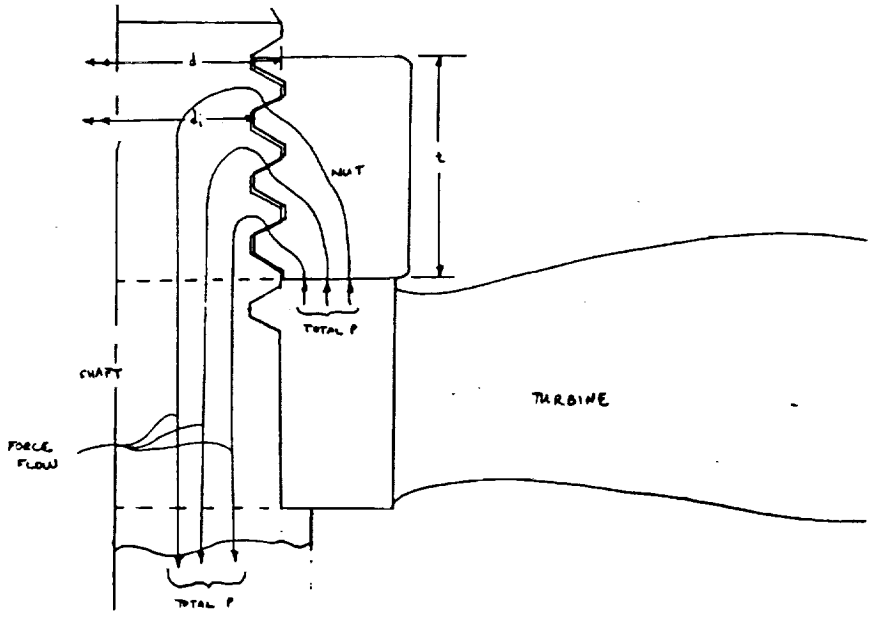

Figure 5

The stresses the shaft and nut under go are determined by equation (2) which can be solved in terms of the maximum allowable diameter of the shaft due to the given loads and material properties.

$$\sigma_y = \frac{4 P p}{\pi (d^2 - d_i^2) t} \qquad \text{equation (2)}$$

Where:

p = Number of threads in contact
P = Thrust load due to turbine
t = Thickness of Nut
d_i = Inner shaft diameter
d = Outer shaft diameter
σ_y = Yield strength (with F.S. = 1.1)

The contact area of the threads had to be reduced due to the use of splines and the difference in diameters, set at 0.0001 m. Manipulating equation (2), we determined an equation in terms of the outer diameter which can be seen as equation (3).

contact area: $\frac{\pi}{8}(d^2-d_i^2)$

$$d = \frac{8Pp}{.0002t\pi\sigma_y} + \frac{1.0*10^{-8}}{.0002} \qquad \text{equation (3)}$$

The allowable diameter for successful operation was found to be 0.00348 m. The actual calculations for this can be found in Appendix D.

TORQUE TRANSFER

The torque induced on the shaft is transmitted from the turbine and hub to the shaft with the use of splines. Splines were chosen because they "can transmit higher torque than a keyed shaft of comparable dimensions."[33] Parallel splines-four spline close fit with the top portion of the spline threaded to allow the nut to be fastened (see Figure 6) was chosen because of the ability to transfer the torque without slip or damage.

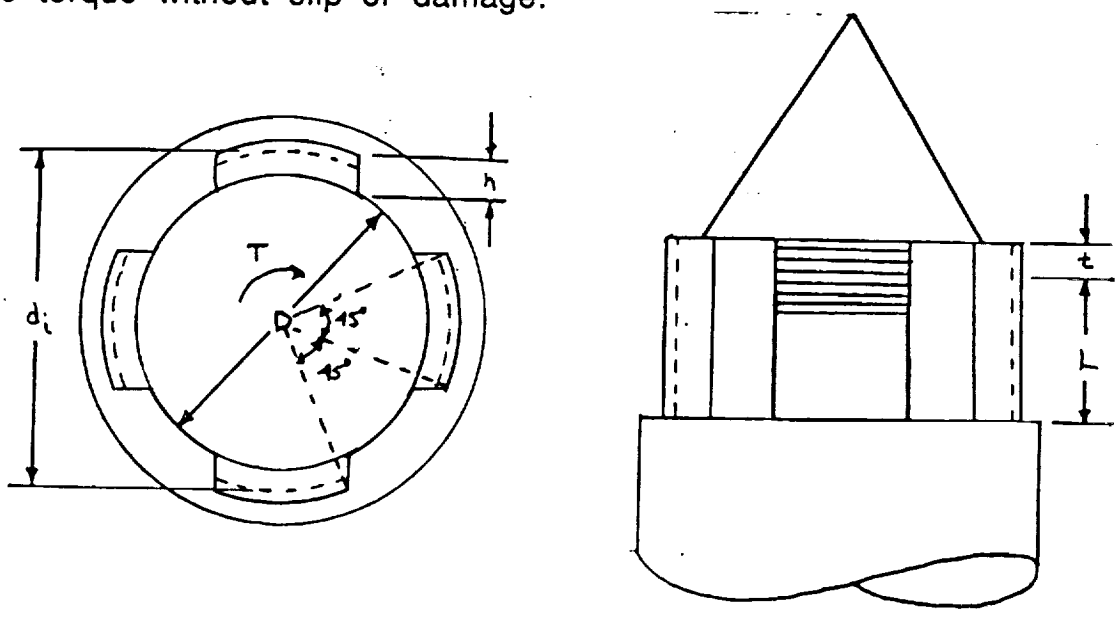

Figure 6

Because "a splined shaft is weaker in torsion than in bending"[33], which our design doesn't have, the torque carrying capacity of a splined shaft would be the size determining force. the torque carrying capacity equation for parallel-side splines can be seen as equation(4).

$$T = i\,(D_m/2)\,Lps \qquad \text{equation(4)}$$

Where:

T = Torque applied
i = Number of splines
L = Effective Length
D_m = Mean Diameter= 0.5(D + di)
p = Permissible side pressure(4* Nominal Shear(t))
s = Contact distance = 0.5(di - D)- 2h
h = Contact surface
D = Inner shaft diameter
di = Outer spline diameter

With manipulation of equation (4) in terms of the governing diameter (D) and plugging in known terms the optimum diameter was found to be 0.00247 m. The actual calculations can be found in Appendix D. The shear force on the splines was also analyzed with the use of equation (5).

$$R = \frac{2T}{Dm} = \frac{4T}{(di + D)} \qquad \text{equation (5)}$$

Where:

R = Shear force on splines
T = Torque applied by turbine hub

The shear force was found to be much smaller than the ultimate shear force,with a Factor of Safety of 1.1, so the splines do not fail in shear. Analysis for this can be found in Appendix D.

SHAFT ANALYSIS

The design of the shafts main-body diameter is only controlled by the torque applied by the turbine and the possible detrimental

effects due to the drastic changes in temperature on Mars which could cause elongation or shrinkage problems. In determining the diameter forced by the torque equation (6) was used and solved in terms of the diameter, equation (7).

$$T = \frac{J\tau}{c} \qquad \text{equation (6)}$$

$$D^3 = \frac{16\,T}{\pi\,\tau} \qquad \text{equation (7)}$$

Where:

T = Torque applied by turbine
J = Polar moment of inertia
c = Diameter /2
τ = Maximum shear stress
D = Shaft diameter

In computing the minimum allowable diameter it was found to be 0.00253 m. The analysis can be found in Appendix D. The next most important factor to evaluate was the elongation or shrinkage of the shaft due to the large range of temperatures on Mars. Using the coefficient of thermal expansion, the known temperature range, and the length the maximum change in length was calculated using equation (8), and found to be 0.00045 m. This is insignificant since in our design the turbine has 0.015 m of lift off of the lip and the calculated change would have little effect on the overall operation.

$$\delta = \alpha\,(\Delta T)\,L \qquad \text{equation (8)}$$

Where:

ΔT = Temperature change
L = Overall length
δ = Change in length
α = Coefficient of thermal expansion

FINAL DESIGN OF SHAFT ASSEMBLY

Once all of the design features were analyzed with each type of load it would experience the final step in the design of the shaft assembly could be done. All of the governing diameters computed could be compared and the largest would have to be the governing design diameter. With this technique some of the features may have a larger diameter than required but all of the features and shaft would be failure free. The resulting design can be seen in Figure 7

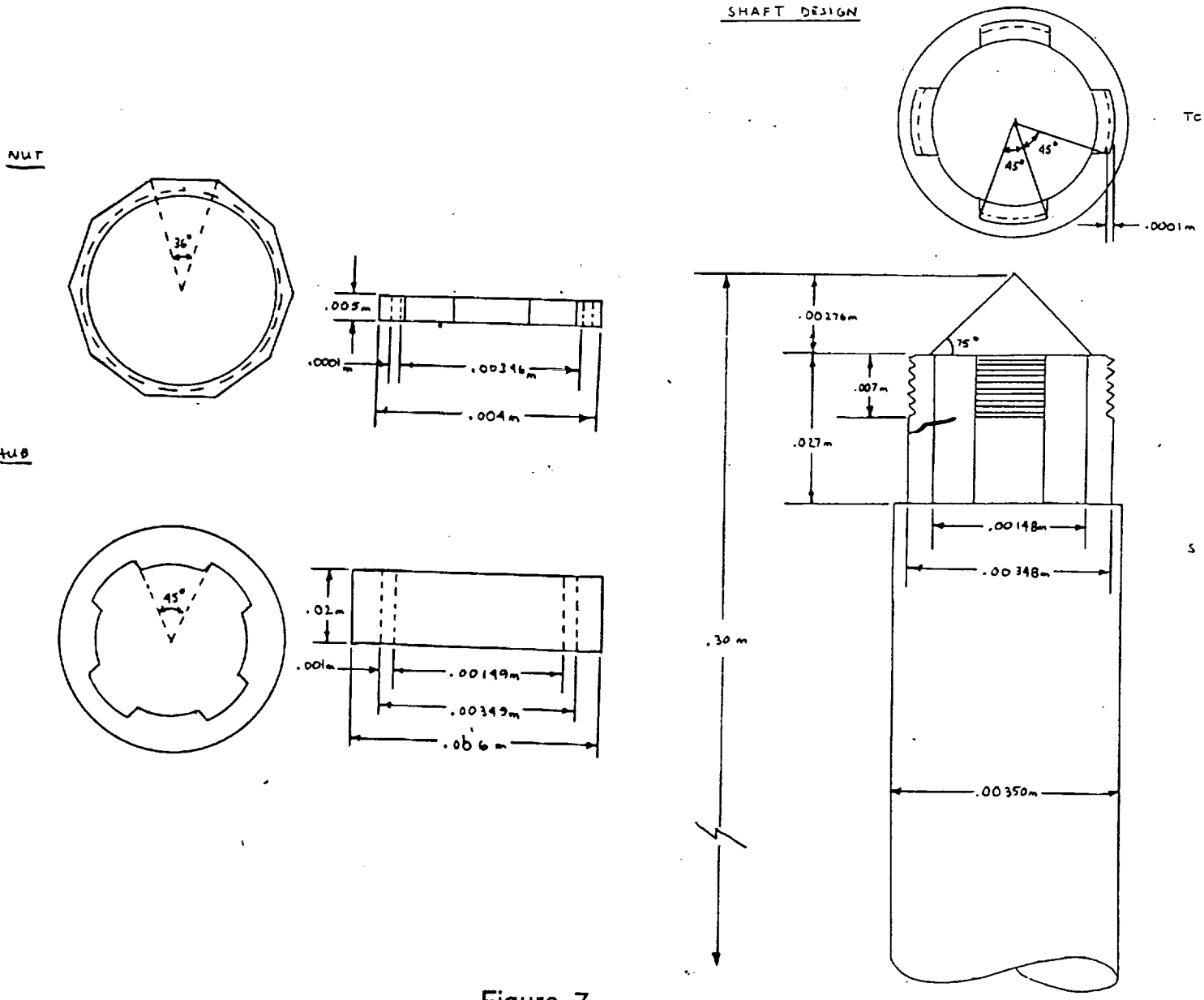

Figure 7

JEWEL BEARINGS

Jewel bearings ~~are just as the name suggests, they~~ are ~~bearings~~ made ~~with jewels~~ of materials such as; diamonds, sapphires, rubies, etc. We selected conical diamond jewel bearings to be placed in titanium cones. The reason we selected to use jewel bearings is for their comparable high strength, but most importantly, because they have almost no friction and require no lubrication during use. The friction factor is a great one because we are working with such small forces a large friction force would damp and destroy the work input. ~~It is also important because~~ this is the only moving part and ~~most~~ losses will occur here. The higher the efficiency of this part the better the end result. Finally, a specification of no contaminates justifies ~~the lack of~~ need for no lubricants, and eases design.

MASS ANALYSIS

As in all NASA designs a complete mass analysis has to be done. The mass analysis is the calculation of all the individual components masses. In the case of the shaft assembly the masses of the following components were computed.

Component:	Weight	Mass
-Main shaft body	0.042 N	0.011 kg
-Conical tips	5.2×10^{-5} N	1.39×10^{-5} kg
-Splines	0.0032 N	8.5×10^{-4} kg
-Reverse thread nut	0.00026 N	6.9×10^{-5} kg
-Wire bearing supports	8.6×10^{-7} N	2.3×10^{-7} kg
-Jewel Bearings	6.2×10^{-6} N	1.6×10^{-6} kg
-Aluminum hub	0.0047 N	0.0013 kg
Totals	0.0491 N	0.0119 kg

All the components were made of titanium except for the hub which was made of aluminum. The reason for this is that the turbine blades are made of aluminum and for welding proposes so was the hub. Their respective densities are 4373 kg/m^3 and 2768 kg/m^3. The mass is computed in terms of Martian acceleration of gravity which is 3.73 m/sec2. All calculations of mass and weight of the components can be found in Appendix D.

ROTOR DESIGN

INTRODUCTION

One of the most critical parts in a windmill is the rotor. The rotor is made up of several blades fastened to a central hub. This assembly absorbs the winds energy and transforms it into work which is transformed into power. In the following sections I will describe the process used in designing the tornado vortex windmill rotor. I will cover some airfoil theory, airfoil selection, tip speed selection, Airfoil chord selection, airfoil characteristics, airfoil analysis, and mass analysis.

AIRFOIL THEORY

The main feature of the rotor is its blades. The blades are the windmills direct link to the kinetic energy in the air. A good understanding of airfoil characteristics will lead to an efficient transfer of energy. Basically I would like to introduce some commonly used terms and their definitions. Below is the standard setup of an airfoil cross section.

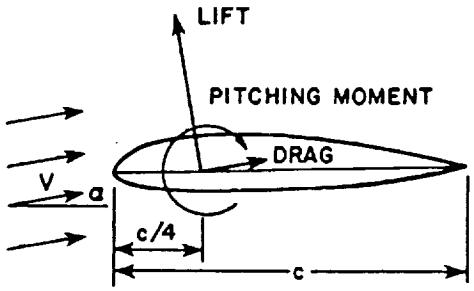

Definitions:

- V= Wind velocity relative to the airfoil.
- c= Chord length, the distance from the tip to the tail of the airfoil
- α= Angle of attack. This is the angle between the relative wind velocity and chord line
- c/4= Quarter chord point
- L= Lift force
- D= Drag force
- b= Wing Span. Length of wing in axial direction

The main assumption used is two dimensional flow. This assumption fits our model very well because our rotor is positioned in a cylindrical region and this positioning prevents any flow from escaping around the tips of the airfoil. Other important values are coefficient of lift, coefficient of drag, and coefficient of moment whose definitions are:

$$C_l = L/0.5\rho V^2 cb$$
$$C_d = D/0.5\rho V^2 cb$$
$$C_m = M/0.5\rho V^2 c^2 b$$

To determine which airfoil is best we look at the coefficient of drag verses coefficient of lift curves. By drawing a line from the origin and tangent to the curve we can find which curve has the largest lift/drag ratio. In wind turbine design the maximum L/D ratio gives the best angle of the resultant aerodynamic force vector for the generation of torque. Thus we want the airfoil cross section that best fits our requirements.

AIRFOIL SELECTION

It seems obvious that the best airfoil will be the one with its Cd verses Cl curve low and to the right. Yet there are so many airfoil cross section types. It would be difficult to determine which type of airfoil best fits our situation. In order to make our airfoil selection less random I used a table of windmill specification to direct my search. From this table (see Appendix E) I found that the NACA 23000 type airfoil was the most commonly used. Using this data as a guide I decided to use the NACA 23000 series and the various curves are located in the Appendix E. To determine which of the 23000 series airfoils had the largest L/D ratio, I used the method previously described(Draw a line from the origin tangent to the curve). I then took the values at the tangent point and put them in a table for comparison. It turned out that airfoil 23012 had the largest L/D ratio so it obviously was the selected airfoil of our design. The resulting critical values are:

airfoil type = NACA 23012
coefficient of lift =0.88
coefficient of drag =0.0144
angle of attack =7.0 degrees

Note that this is the angle of attack that we must maintain in order to keep our coefficients of lift and drag constant.

TIP SPEED SELECTION

Although a blade tip speed selection may seem trivial it is a rather important parameter in designing the twist of the airfoil. Usually the tip speed is related to a generators working angular velocity but because we do not have a generator to work from I tried to make a reasonable guess. I based my "guess" on the previously mentioned windmill table, a previously tested vortex windmill, and suggested rpm values from a wind turbine engineering design book. From these sources I limited my tip speed to a range of rpms (1000-7200) with the tip speed equation being.

$X = \Omega R/V$

X-The tip speed ration
W-angluar velocity of rotor
V-turbine wind inlet velocity
R-turbine radius

Looking at source[31] there is a noticeable increase in turbine efficiency in the tip speed ratio range of three to six. From our final calculations we found that the turbine radius was 0.11 meters. From all this data I was able to further optimize the rpm range to (1953-3255 rpm).

AIRFOIL CHORD SELECTION

To determine the airfoils chord length I used a method called Glavert blade element analysis(see Appendix E). This method optimizes the airfoil by a prefered product of chord length and coefficient of lift(C*Cl). The optimum blade layout is given by

$$(B\Omega/8\pi)*Vo*C*Cl=[(4a-1)/(1-2a)]*((1-1)*(1-3a))^{1/2}$$

B=number of Blades
Vo=turbine inlet velocity (approx. 7.5)
a = axial flow induction factor

Once these values are known the equation is solved for C to give us our desired chord length. The problem arises when calculating the induction factor(a). To find the induction factor I used Glavert momentum theory. In this theory it is assumed that small radial sections of the airfoil blades can be analyzed independently. Through a series of equations and manipulations (see Appendix E) we get the equation that

a=Vo-u/V0
Vo=free stream velocity
u=velocity across the turbine

In the common windmill case Vo is greater than u and the resulting(a) value is somewhere between 0.3 to 0.5. We then simply plug it into our equation for chord length and solve. As you already know ours is not a common windmill case. For our case I had to determine(u). I did this with the relationship comparing change in pressure across a disc to pressure change equations derived by source[28]. Working through the number crunching I was left with a very unusual result. It turned out that our velocity across the turbine was actually more than the free stream velocity (see Appendix E). From these results I drew the following possible scenario. For arguments sake lets say that the free stream velocity is 10 m/s. In the common windmill this velocity is decreased due to the extraction of energy by the turbine. In our case we have a vortex on the exhaust side of the turbine so the velocity and the resulting kinetic energy may be being increased to say 20 m/s. The turbine in the meantime is extracting 5 m/s worth of energy. The result is still an increase in the velocity (10 m/s goes to 20 m/s - 5 m/s =15 m/s). because of this unusual result I was forced to assume a value of (0.3 = a). From this I was then able to calculate some chord lengths by choosing three different tip speeds.

AIRFOIL CHARACTERISTICS

With all pertinent data on the airfoil collected. The last phase before I could test for loading was determination of the correct twist of the airfoil. To do this I chose a rpm of 3000 and a chord length of 4.5 cm.

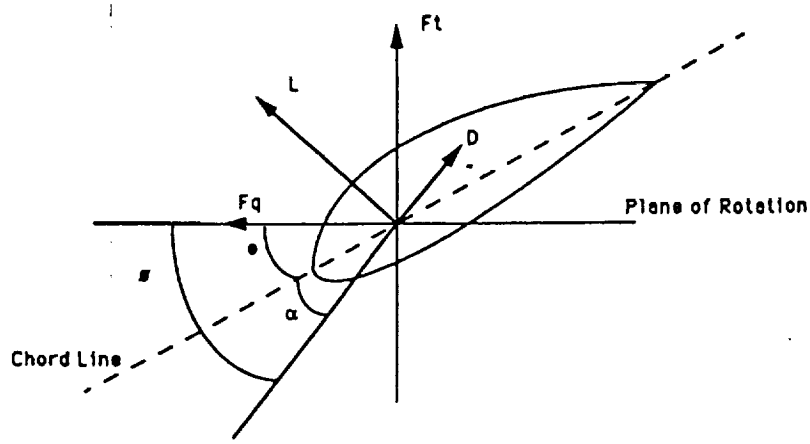

Looking at the figure above, θ represents the angle of twist at each section. The goal is to keep α (angle of attack) constant so that our airfoil stays in the region of maximum Lift/Drag. Assuming the velocity across the turbine remains constant. We see that the governing factor of twist is (Ωr) or the wind velocity component due to the rotation. Using the equation:

$$\tan \phi = u/\Omega r$$

and solving for ϕ. With $\phi = \theta + \alpha$, we solve for ϕ to get $\theta = \phi - 7$ (7 is our set angle of attack) A table of the airfoil characteristics is displayed in a table in the appendix. The resulting angle of twist is given by the curve

$$\theta = 82.567 - 1923.35 + 1.8949E4 * r^2 - 6.8765E4 * r^3$$

AIRFOIL ANALYSIS

To analyze the resulting forces on the airfoil I had to integrate the lift and drag over the span of the blade.(See Appendix E) I then calculated and graphed the thrust force, the torque force, the moment about the x-axis, and the moment about the y-axis. The resultant forces and moments are:

FThrust=0.038 N
FTorque=0.024 N
Mx=0.003 Nm
My=0.001 Nm

The resultant torsional moment about the y axis was not calculated due to the center of pressure being a negligible distance from the axis(the moment arm was less than 1/10 of a millimeter). When looking at the force curves(see Appendix E) the thrust curve increases as we go radially out while looking at the torque force curve the opposite occurs. This phenomena occurs mainly due to the differing drag and lift contributions. Near the center the twist of the wing is very large (70 deg) with the resulting lift force being near horizontal. Thus the large lift force contribution resulting in the large torque force near the center. On the other hand, as we go radially out, the lift force becomes more vertical. Thus the thrust force increases. Once the moments and forces were established I tried to establish what stresses the wing might see. For this step I simplified the cross section of the wing into three sections to find the moment of inertia.(see Appendix E) Then using this with the equation for stress. The maximum stress on the tensile side is obtained. The resultant stress is far bellow the yield stress of the Aluminum 2024-T4.

MASS ANALYSIS

When deciding what material to make the airfoil there was one governing concern. This was the fact that our rotor had a total thrust force of 0.076 Newtons. From the mass analysis of the shaft assembly, and its equivalent weight on Mars of 0.049 Newtons. I was left with a total allowable weight of 0.027 Newtons. Thus the driving force in the material selection was density. This is why I chose Aluminum 2024-T4 . Compared to other common aerospace materials this had the lowest weight while the strength was comparably high(See Appendix E). The resulting mass analysis left me with a total mass of 5.899×10^{-3} kg. The resulting weight on Mars was 0.022 Newtons(for both airfoils).

AEOLIAN EFFECTS

Aeolian transport effects are of major concern on the surface of Mars. Mariner and Viking Orbiters revealed many aeolian features including dunes, yardangs, and various pits and grooves on the Martian surface. "These features appear to be associated with topographical structures, such as craters, and are the result primarily of two major wind directions: off-pole winds that become easterly due to Coriolis forces during summer, and on-pole winds that become westerly during winter."[12]

Although it can be concluded that there is sand on Mars, the characteristics and compositions of the sand particles are questionable. "With the apparent absence of granite on Mars, quartz sand is unlikely to be present. Most investigators feel that the grains could be comminuted basalt."[12] What is certain is that these particles are on average less than 2 μm, and fly faster, higher, and farther on Mars than on Earth. To put this into perspective, the ratio of mass transport on Mars to that on Earth would be about 6.5.[12]

"The maximum abrasion from these sand particles occurs at a height of about 10-15 cm above the ground due to a combination of grain sizes, fluxes, and particle velocities, all of which vary with height and wind speed."[12] The rate of abrasion is substantially higher on Mars than on Earth because of the higher velocities required for particle movement. These high winds result not only in greater particle velocities, but in increased fluxes as well. "Calculations of the present rates on Mars yield values ranging up to 2.1×10^{-2} cm/yr."[12]

In addition to daily winds, Mars also experiences periodic local and global dust storms. Earth-based and spacecraft observations show that major dust storms on Mars typically begin in the southern hemisphere during spring or early summer, when Mars is closest to the Sun. The amount of dust injected into the atmosphere of Mars from these storms is estimated to be about 2.9×10^{15} g/yr, meaning Mars is about 20 times 'dustier' than Earth.[12]

The major dust storms originate in three general areas of Mars: (1) on sloping plains between the northwest rim of the Hellas basin and the uplands of Noachis, (2) sloping plains to the west, south, and southeast of Claritas Fossae, and (3) on the low-lying region of Isidis Plantitia, east of Syrtis-Major. All three areas are in sub-tropical latitudes and constitute large east-facing slopes where one would expect differential heating to occur.[12]

Global dust storms cover nearly the entire planet and in some cases blanket Mars completely. These storms can last anywhere from 90 to 175 days, and average wind speeds can reach upwards of 65 m/sec.

max speeds = ?

Although Viking Orbiters observed only about 1% of the planet's surface each day, many local dust storms were recorded. According to Viking data, there were 16 local dust storms occurring in 1977, which means there were probably many more during that time.[12] Again, most of the local dust storms observed by the Viking Orbiters occurred during spring and early summer in the southern hemisphere. In general, local dust storms appear to be random in their occurrence, but tend to be associated with local slope winds and along the edges of the south polar cap where strong thermal gradients are found.

Aeolian processes appear to be a dominating process currently active on the surface of Mars and may significantly effect the performance of the Martian Tornado Vortex Wind Generator. By strategically placing the wind generator away from topographical features such as craters, we may be able to keep aeolian effects to a minimum. "In addition, studies of aeolian transport of Martian sand particles indicate that it would take about five years for accumulated sand to build up to potentially clogging level which could cause failure.[27]

Good Analysis

EXPERIMENTAL & THEORETICAL RESULTS

The Martian Tornado Vortex Wind Generator does not have any concrete performance data at this time. However, data for similar tornado-type wind energy systems has been compiled by Eric Jacobs of the Solar Energy Research Institute in Golden, Colorado. The results are briefly highlighted below.

EXPERIMENTAL RESULTS

The maximum or peak power coefficients, determined experimentally by Yen, Hsu and Ide for various tower configurations are shown in Table 2.

Table 2 [18]

	Tower Shape	Turbine	Radial Inflow	D(m)	H/D	D_t/D	$C_{p,max}$
Yen	Spiral	Screens	no	0.25	2.1	0.30	0.06
Yen	Spiral	Bladed	no	0.25	2.1	0.40	0.18
Hsu & Ide	Circular	Screens	no	0.36	1.6	0.29	0.08
Hsu & Ide	Circular	Screens	yes	0.36	1.6	0.29	0.15
Hsu & Ide	Spiral	Screens	no	0.48	1.2	0.21	0.22
Hsu & Ide	Spiral	Screens	yes	0.48	1.2	0.21	0.26
Yen	Multivane	Bladed	no	0.25	2.0	0.40	0.11
Yen	Multivane	Bladed	no	0.61	2.0	0.33	0.08

The discrepancies between the respective tests of each tower are due to the differences in the model geometries. Yen's multi-vane tower results should be reduced to reflect the use of ram air inlets which artificially increases the amount of wind entering the tower. "These results demonstrate the marked reduction in the power coefficients found with the multi-vane tornado-type wind models, indicating that use of an omnidirectional tower may induce a significant performance penalty relative to unidirectional designs such as the spiral configuration. However, an omnidirectional tower design would be necessary to permit use of winds from all directions."[18]

THEORETICAL RESULTS

Several theoretical studies have attempted to analyze the coefficient of performance of tornado-type wind models. A numerical solution was performed by Ayad[4] in which he predicted a maximum power coefficient, $c_{p,\ max}$ of approximately 0.20 for H/D = 1 and D_t/D = 0.4. "The mathematical solutions for tornado-type wind energy systems derived by Yen, Hsu, Ide and others, are all dependent on several underlying assumptions, idealizations, and/or approximations. These include assumed tower inlet velocity profiles, laminar and/or radially unbounded vortex flow, and assumed vortex velocity profiles. Also the turbine wake-vortex interaction is generally neglected as insignificant or unsolvable."[18]

COMPARISON WITH MOD-2

The MOD-2 is a horizontal axis wind turbine designed by Boeing Engineering. Optimistically a peak system c_p of 0.20 might be attainable from a tornado-type vortex system. In comparison the MOD-2 has a peak system c_p of-0.375. In addition, the tornado-type vortex system would need to be nearly twice the size as the MOD-2 to produce the same amount of net power output.

RECOMMENDATIONS & CONCLUSIONS

As was stated earlier, most of the work done on Tornado Wind Energy Systems was done in the late 70s and early 80s during the energy crisis, and has since then ceased. In concept a Tornado Vortex Generator holds much promise. However it can be shown experimentally and theoretically that tornado-type wind energy systems are actually inferior to modern day wind machines such as the savonis and derrius wind machines. Therefore we conclude that a tornado-type vortex generator is not the most feasible method for extracting power from Martian winds. We also recommend that a different approach be taken to finding the best possible solution for long-life, low powered Martian surface probes, possibly savonis and derrius wind machines, or even a electrofluid dynamic (EFD) wind driven generator.

REFERENCES

1. Abbott I., and Von Doenhoff A., Theory of Wing Sections, Dover Publications, New York, 1959.

2. Allen D., and Haisler W., Introduction to Aerospace Structural Analysis, John Wiley & Sons, New York, 1985.

3. Arndt et al, "Martian Egg Probe Design," Engineering Mechanics Senior Design Project, May 1989.

4. Ayad S.S., "A Numerical Model for the Flow Within the Tower of a Tornado-type Wind Energy System," Journal of Solar Energy Engineering, Vol. 103, No. 4, Nov. 1981.

5. Beer F.P., and Johnston R.E., Mechanics of Materials, McGraw-Hill Book Company, New York, 1981.

6. "Boron for Aerospace Structures," Materials Engineering, July 1989.

7. Boston P.J., The Case for Mars, AAS Science and Technology Series, Vol. 57, 1984.

8. Buck M.E., "High Strength & Modulus Filaments of Boron & Silicon Carbide," Materials & Design, Vol. 8, No. 5, Sept./Oct. 1987.

9. Cook R.D., and Young W.C., Advanced Mechanics of Materials, Macmillan Publishing Company, New York, 1985.

10. Eggleston D., and Stoddard F., Wind Turbine Engineering Design, Van Nostrand Reinhold Company, New York, 1987.

11. Gipe P., "VAWT's: A Brief Introduction," Wind Power Digest, Spring 1980.

12. Greeley R., and Iverson J., Wind as a Geological Process: on Earth, Mars, Venus, and Titan, Cambridge University Press, Cambridge, England,1985.

27. Ralston M., "MARS L.A.M.P.-A Design Proposal for a Mars Wind Energy Conversion System," Engineering Mechanics Design Project, 1990.

28. Rangwalla A.A., and Hsu C.T., "Performance and Flow Analysis of Vortex Wind Power Turbines," ISU-ERI-Ames 83098, Iowa State University, Ames, Iowa.

29. Roberson J., and Crowe C., Engineering Fluid Mechanics, Houghton Mifflin Company, Boston, 1985.

30. "TARP," Wind Power Digest, Spring 1980.

31. Yen J.T., "Investigations of the Tornado Wind-Energy System," DOE/ET/20022--T1, Grumman Aerospace Corporation, Bethpage, New York, May 1980.

32. Zorich R, "The Betz Equation," Wind Power Digest, Vol. 25, Fall 1982.

33. Mechanical Design and Systems Handbook.

APPENDICIES TABLE OF CONTENTS

APPENDIX A

DESIGN SCHEDULE..... A-1
NEEDS/FUNCTIONS LIST..... A-2
FAST DIAGRAM..... A-4

APPENDIX B

SECONDARY CALCULATIONS..... B-1
MMC ADVANTAGES & DISADVANTAGES..... B-4
PRIMARY CALCULATIONS..... B-6
BASE ANALYSIS..... B-13
SUPPORTS
BUCKLING
THERMAL EXPANSION
MASS ANALYSIS..... B-26

APPENDIX C

VANES AND TOWER SELECTION..... C-1
STRESS ANALYSIS
IMPACT FORCE..... C-5
COMPRESSIVE STRESS..... C-5
BUCKLING TEST..... C-6
WIND DRAG AND SHEAR STRESS..... C-8
STABILITY..... C-14
FINAL DESIGN..... C-13
MASS ANALYSIS..... C-16

APPENDIX D

MATERIAL SELECTION..... D-1
THREAD ANALYSIS..... D-3
SPLINE ANALYSIS..... D-5
SHAFT ANALYSIS..... D-8
JEWEL BEARING SUPPORT..... D-10
FINAL DESIGN..... D-11
MASS ANALYSIS..... D-12

APPENDIX E

ACTUATOR DISC THEORY..... E-1
INITIAL CALCULATIONS PART I..... E-8
INITIAL CALCULATIONS PART II..... E-19
AIRFOIL THEORY..... E-19

AIRFOIL CURVES..... E-23
TIP SPEED RATION..... E-29
AIRFOIL CHORD SELCETION..... E-31
AIRFOIL CHARACTERISTICS..... E-36
AIRFOIL ANALYSIS..... E-38
MASS ANALYSIS..... E-49
FINAL CONFIGURATION..... E-51